Experimental Demonstration of an Indoor Positioning System Based on Artificial Neural Network

[1]Bangjiang Lin, [2]Qingyang Guo, [1]Chun Lin, [1]Xuan Tang, [1]Zhenlei Zhou and [3]Zabih Ghassemlooy

[1]Quanzhou Institute of Equipment Manufacturing, Haixi Institutes, Chinese Academy of Sciences, Quanzhou, China, Corresponding email: linbangjiang@fjirsm.ac.cn, xtang@fjirsm.ac.cn.

[2]Department of Electronic Information, School of Electronic and Information Engineering, Tongji University, China.

[3]Optical Communications Research Group, Faculty of Engineering and Environment, Northumbria University, U.K.

Abstract: We propose a 2D visible light positioning system based on artificial neural network (ANN), where the light emitting diodes (LEDs) are grouped into blocks and the block coordinates are encoded with under-sampled modulation. A camera is used to decode the block coordinate in the receiver. The receiver's position is approximately and precisely estimated using the decoded block coordinate and a typical back propagation ANN, respectively. The experimental results show that the proposed scheme offers a mean positioning error of 1.49 cm.

Index Terms: Visible light communications (VLC), artificial neural network (ANN), optical camera communications (OCC), indoor positioning.

1. Introduction

In recent years, indoor positioning systems (IPSs) have attracted a lot of attention. There are various indoor positioning technologies proposed such as Radio-Frequency

Identification (RFID), Ultra-Wideband (UWB), and Wi-Fi [1-4]. However, these methods suffer from electromagnetic interference and high cost. Visible light communications (VLC) based on white light emitting diodes (LEDs) can be utilized for both lighting and communications simultaneously. IPSs using VLC have recently gained popularity as effective alternatives to the traditional techniques due to the advantages such as high positioning accuracy, license-free operation, no electromagnetic interference and low-cost frontends [5-7]. Both camera and photo-detector (PD) can be used as a receiver (Rx) to detect the optical signal transmitted by LEDs. In the PD-based VLC-IPS, the distance or the angle between the transmitter (Tx) and the Rx is calculated by the received signal strength (RSS), time of arrival (TOA) and time difference of arrival (TDOA) techniques. Perfect synchronization between the Tx and the Rx is required for TOA and TDOA [8]. In RSS, in order to accurately estimate the distances, the optical Rx needs to receive signals from multiple Txs with no interference [9-13]. To address this problem, frequency domain division multiplexing and time domain division multiplexing were proposed in [9, 13] and [10, 12], respectively. In the camera based VLC-IPS, the Rx's position is determined based on the coordinates of LEDs in the real world and in the captured image [14-16]. In [14], both the Rx's position and direction were measured using an image sensor (IS). In [16], we experimentally demonstrated an IPS based on optical camera communications (OCC) with low PE.

Machine learning as a powerful tool has been widely used to solve a range of problems in different applications [17] such as data mining, pattern recognition, medical imaging, artificial intelligence, etc. Recently, machine learning have been

adopted in optical communications for optical signal-to-noise ratio (OSNR) monitoring, modulation formats identification, nonlinearity mitigation, etc. [17-21]. In this paper, we propose a VLC-IPS based on artificial neural network (ANN) and OCC, where the LEDs are grouped into blocks and the block coordinate is encoded on a single LED per block. A camera is used to decode the block coordinate. The Rx's position is roughly estimated using the decoded block coordinate. Then a trained back propagation (BP) ANN is used to precisely estimate the Rx's position. The feasibility of the proposed scheme is experimentally verified. The experimental results show that the proposed IPS offers a mean positioning error (PE) of 1.49 cm. The PE is defined as the distance difference between the reference and estimated points.

The rest of the paper is organized as follow: Section 2 describes the proposed indoor positioning scheme in detail. Section 3 presents the experiment setup and results followed by the concluding remarks in Section 4.

2. Proposed system for indoor positioning

Fig. 1 shows the block diagram of the proposed scheme. We assume that LEDs are distributed evenly on the ceiling. Every 4 LEDs are grouped into a block. One LED per block is encoded with the coordinate information of the block center. The transmitted coordinate data is encoded with under-sampled modulation and captured by a camera. The detail working flow of the OCC can be found in [16]. The Rx's position is firstly calculated from the decoded block coordinate. A typical BP ANN is used to acquire more accurate position, which is composed of the input, the hidden and the output layers as shown in Fig. 2. The inputs of the neural network are the

center point coordinate (i.e., (x', y')) of the block in the image. The outputs are the coordinates of the Rx (i.e., (x, y)) in the real world, and there are N nodes in the hidden layer. The ANN can be divided into training and trained stages. In the training stage, several sets of inputs and outputs are used, and the object of the training is to minimize the sum of the squared errors between the actual and the desired output values. After the training, with any meaningful inputs to the trained artificial neural network, corresponding outputs can be obtained.

It should be pointed out that, it is not possible to capture the image of all the 4 LEDs when the Rx is placed on the edge of the blocks. We propose a simple movement-based method to overcome this problem, in which the Rx's position is determined based on its previous three positions. The current position (x_t, y_t) of the Rx is given by:

$$\begin{cases} y_t = l_t \times \sin(\arctan(k_t)) + y_{t-1} \\ x_t = l_t \times \cos(\arctan(k_t)) + x_{t-1} \end{cases}, \tag{1}$$

where (x_{t-1}, y_{t-1}) is the Rx's position at t-1 time. l_t is given by

$$\begin{cases} l_{t-1} = \sqrt{(x_{t-1} - x_{t-2})^2 + (y_{t-1} - y_{t-2})^2} \\ l_{t-2} = \sqrt{(x_{t-2} - x_{t-3})^2 + (y_{t-2} - y_{t-3})^2} \\ l_t = (l_{t-1} + l_{t-2})/2 \end{cases}, \tag{2}$$

where (x_{t-2}, y_{t-2}) and (x_{t-3}, y_{t-3}) are the Rx's positions at t-2 and t-3 times, respectively, and k_t is given by:

$$\begin{cases} k_{t-1} = \dfrac{x_{t-1} - x_{t-2}}{y_{t-1} - y_{t-2}} \\ k_{t-2} = \dfrac{x_{t-2} - x_{t-3}}{y_{t-2} - y_{t-3}} \\ k_t = 2k_{t-1} - k_{t-2} \end{cases}. \tag{3}$$

3. Experiment Setup and Results

The feasibility of the proposed scheme is experimentally demonstrated as shown in Fig. 3. For the selected block, its center coordinate is encoded and transmitted via LED4. The coordinate data is encoded into under-sampled phase shift keying (UPSK) symbols as shown in Fig. 4(a) and then uploaded to an arbitrary waveform generator (AWG) operating at 0.1-MS/s. The UPSK signals $s(t)$ can be expressed as:

$$s(t)=\begin{cases}\mathrm{sgn}\left(\cos(2\pi f_h t)\right), 0<t<=T_c \quad n=1\\ \mathrm{sgn}\left(\cos(2\pi f_s t+a_n\cdot\pi)\right), (n-1)T_c<t<=nT_c \;\; n>1\end{cases}, \tag{4}$$

where the first bit (i.e. n=1) is used to identify the beginning of each data frame, which is a square wave signal with a frequency of f_h. f_h is much higher than the frame rate f_c. The binary data bits (i.e. a_n) are encoded with a square wave signal with a frequency of f_s. In order to frequency-synchronize the Tx and the camera (i.e., the Rx), we set $T_c=f_c^{-1}$ and $f_s=4f_c$. The output of AWG (i.e., the UPSK signal) is direct current (DC)-level shifted prior to intensity modulation of LED4. At the Rx, a camera (Canon EOS 7D Mark II) is used to detect the transmitted signal. Fig. 4 (b) depicts the schematic block diagram of the decoder at the Rx, where a hard threshold decision with two threshold (TH) levels are adopted to identify the states (i.e., the RGB values of the LED4). If the RGB value is ≥ TH1 then it is identified as 1. If the RGB value is ≥ TH2 and < TH1 then it is classified as the first bit of a frame, else it is identified as 0. The decoded coordinate is used to determine the approximate position of the Rx. In the offline stage, 289 points on the receiver plane are sampled evenly and the coordinate of the block center in the image is calculated at these points. Then the

coordinates of the block center in the image (i.e., (x', y')) and the Rx (i.e., (x, y)) of these points are treated as inputs and outputs, respectively, and used to train the artificial neural network until the sum of the squared error of these sampled points is minimized. In the positioning stage, the approximate position of the Rx is firstly determined by the decoded block coordinate. Note that the transmitted block coordinate is decoded by the camera. The captured image of the block is processed by the trained neural network. The output of the ANN is the precise position of the Rx. If the camera cannot capture more than 2 LEDs in the image, the proposed movement-based method is used to determine the precise position, as processed by the equations (1)-(3). The detail process for the proposed scheme is shown in Fig. 5. To determine the position, the online processing time is 0.15s. All the key system parameters are provided in Table I.

Fig. 6 depicts the mean PE as a function of the number of nodes in the hidden layer. The PE is given by:

$$D_{error} = \sqrt{(x - x_e)^2 + (y - y_e)^2}. \quad (5)$$

where (x, y) and (x_e , y_e) are the coordinates of the reference and estimated points, respectively. The PE decreases with the increasing number of nodes. The decreased value of PE is small. Fig. 7 depicts the estimated as well as reference positions for the proposed IPS. The number of nodes in the hidden layer is 15. The maximum and the average PEs are 3.72 cm and 1.49 cm, respectively. Table II shows the PEs for different VLC based positioning systems. All the listed works are with experimental demonstration. In the TDOA based scheme, a synchronized real local oscillator (RLO) at the receiver side is required to calculate the TDOA value which is complicated and

expensive for indoor positioning applications. In the RSS scheme, carrier allocation is proposed to eliminate the interference between the adjacent LEDs. The carrier allocation method would be very complicated in a large place where many LEDs are deployed in the ceiling. Compared with the PD based VLC-IPS, the camera based VLC-IPS is more suitable for indoor positioning, since the camera can be easily integrated in a smart phone. The image processing algorithm can be realized easily using the smart phone. Compared with the image processing methods proposed in [15] and [16], our proposed method offers lower PE and comparable complexity. Similar to the fingerprinting based positioning scheme [22], offline ANN training is required in our proposed scheme. What's more, to ensure successfully positioning, the camera should not be tilted. A tilted angle may cause a large PE. As shown in Table III, the PE increases at a much higher rate with the increase in tilted angle. In the future, we will develop an ANN based 3-D positioning system to address this issue, in which the geometric relations between the objects' 3D positions in the real world and their 2D positions on their projections on the image sensor are used to determine the position.

4. Conclusion

In this paper, we proposed a visible light positioning system based on ANN and OCC, where LEDs were grouped into blocks and the block coordinates were encoded with under-sampled modulation scheme. The position of the receiver was roughly and precisely estimated based on the detected block coordinate and the BP ANN, respectively. We showed that the proposed scheme offered a mean positioning error of 1.49 cm, which was lower compared with other RF-based positioning schemes. The

positioning accuracy depended on the training samples and the convergence of the ANN.

Acknowledgment

This work was supported in part by the National Natural Science Foundation of China under Grant 61601439 and 61501427, in part by the Chunmiao Project of Haixi Institutes, Chinese Academy of Sciences, in part by Fujian Natural Science Foundation under Grant 2017J05111, in part by External Cooperation Program of Chinese Academy of Sciences under Grant 121835KYSB20160006, in part by Development of Scientific Research Instrument of Chinese Academy of Sciences under Grant YJKYYQ20170052, in part by State Key Laboratory of Advanced Optical Communication Systems and Networks, China.

References

[1] Rida, Mohamed Er, et al. "Indoor Location Position Based on Bluetooth Signal Strength." International Conference on Information Science and Control Engineering IEEE, 2015:769-773.

[2] Yang, Chouchang, and H. R. Shao. "WiFi-based indoor positioning." Communications Magazine IEEE 53.3(2015):150-157.

[3] Lin, Xin Yu, et al. "A mobile indoor positioning system based on iBeacon technology." Engineering in Medicine & Biology Society Conf Proc IEEE Eng Med Biol Soc, 2015:4970.

[4] Huang, Chung Hao, et al. "Real-Time RFID Indoor Positioning System Based on Kalman-Filter Drift Removal and Heron-Bilateration Location Estimation." IEEE Transactions on Instrumentation & Measurement 64.3(2015):728-739.

[5] Ghassemlooy, Z., Alves, L. N., Zvanovec, S., and Khalighi, M-A.: Visible Light Communications: Theory and Applications, CRC June 2017.

[6] Hassan, Naveed Ul, et al. "Indoor Positioning Using Visible LED Lights:A Survey." Acm Computing Surveys 48.2(2015):1-32.

[7] Kim, Hyun Seung, et al. "Three-Dimensional Visible Light Indoor Localization Using AOA and RSS With Multiple Optical Receivers." Lightwave Technology Journal of 32.14(2014):2480-2485.

[8] Pengfei Du, et al, "Demonstration of a Low-Complexity Indoor Visible Light Positioning System Using an Enhanced TDOA Scheme." IEEE Photonics Journal 10.4 (2018): 7905110.

[9] Kim, Deok Rae, et al. "An Indoor Visible Light Communication Positioning System Using a RF Carrier Allocation Technique." Journal of Lightwave Technology 31.1(2012):134-144.
[10] Yang, Se Hoon, et al. "Visible light based high accuracy indoor localization using the extinction ratio distributions of light signals." Microwave & Optical Technology Letters 55.6(2013):1385-1389.
[11] Yang, Se Hoon, et al. "Reduction of optical interference by wavelength filtering in RGB-LED based indoor VLC system." Opto-Electronics and Communications Conference IEEE, 2011:551-552.
[12] Hou, Yinan, et al. "Multiple access scheme based on block encoding time division multiplexing in an indoor positioning system using visible light." IEEE/OSA Journal of Optical Communications & Networking 7.5(2015):489-495.
[13] Lin, Bangjiang, et al. "Experimental Demonstration of an Indoor VLC Positioning System Based on OFDMA." IEEE Photonics Journal 9.2(2017):1-9.
[14] Jena, R., S. Price, and J. Gillard. "High-accuracy positioning system using visible LED lights and image sensor." Radio and Wireless Symposium IEEE, 2008:439-442.
[15] Yiwei Li, et al, "A VLC Smartphone Camera Based Indoor Positioning System." IEEE Photonics Technology Letters 30.13(2018):1171-1174.
[16] Lin, Bangjiang, et al. "An Indoor Visible Light Positioning System Based on Optical Camera Communications." IEEE Photonics Technology Letters 29.7(2017):579-582.
[17] Khan, F. N., et al. "Joint OSNR monitoring and modulation format identification in digital coherent receivers using deep neural networks." Optics Express 25.15(2017):17767.
[18] Wang, Danshi, et al. "Nonlinear decision boundary created by a machine learning-based classifier to mitigate nonlinear phase noise." European Conference on Optical Communication IEEE, 2015:1-3.
[19] Christian G. Schäeffer, et al. "Machine Learning Techniques in Optical Communication." Journal of Lightwave Technology 34.6(2016):1442-1452.
[20] Zibar, Darko, et al. "Machine Learning Techniques for Optical Performance Monitoring from Directly Detected PDM-QAM Signals." Journal of Lightwave Technology PP.99(2017):1-1.
[21] Giacoumidis, Elias, et al. "Nonlinear inter-subcarrier intermixing reduction in coherent optical OFDM using fast machine learning equalization." Optical Fiber Communications Conference and Exhibition IEEE, 2017:W3J.2.
[22] S. Feng, X. Li, R. Zhang, M. Jiang, and L. Hanzo, “Hybrid positioning aided amorphous-cell assisted user-centric visible light downlink techniques,” IEEE Access, vol. 4, pp. 2705–2713, 2016.

Biographies

Bangjiang Lin received the B.S. and Ph. D degrees from Electronics Engineering Department of Peking University, China in 2010 and 2015, respectively. He is now an Associate Professor at Quanzhou Institute of Equipment Manufacturing, Haixi Institutes, Chinese Academy of Sciences. His current research interests include passive optical network and visible light communications.

Qingyang Guo is now working toward the B.S. degree in Department of Electronic Information, School of Electronic and Information Engineering, Tongji University, China. He is also a visiting student in Quanzhou Institute of Equipment Manufacturing, Haixi Institutes, Chinese Academy of Sciences.

Chun Lin received his B.S. degree from Jimei University, China, in 2015. He is currently working toward his M.S. degree in Quanzhou Institute of Equipment Manufacturing, Haixi Institutes, Chinese Academy of Sciences, China.

Xuan Tang received her Ph.D. degree and post-doctoral from Northumbria University and Tsinghua University, respectively. She is currently a professor at Quanzhou Institute of Equipment Manufacturing, Haixi Institutes, Chinese Academy of Sciences, China. Her research interests include optical network and visible light communication.

Zhenlei Zhou received his B.S. degree from Luoyang Normal University, China, in 2016. He is currently working toward his M.S. degree in Quanzhou Institute of

Equipment Manufacturing, Haixi Institutes, Chinese Academy of Sciences, China. His research interests include optical network and VLC.

Zabih Ghassemlooy received his B.S. degree from the Manchester Metropolitan University, Manchester, U.K., in 1981, and the M.S. and Ph.D. degrees in optical communications from the University of Manchester Institute of Science and Technology (UMIST), Manchester, in 1984 and 1987, respectively. He is now a professor at the Faculty of Engineering and Environment, Northumbria University, Newcastle, U.K.

Figure captions

Fig. 1. System block diagram.

Fig. 2. Structure of an artificial neural network.

Fig. 3. Experiment setup for the proposed IPS based on OCC and ANN.

Fig. 4. Block diagram of: (a) coder, and (b) decoder.

Fig. 5. The flow chart for determining the position in the proposed system.

Fig. 6. The mean PE versus the number of nodes in the hidden layer.

Fig. 7. The final estimated positions using our proposed scheme.

TABLE I. System Parameters

Parameter	Value
LED	
• Bandwidth	< 5 MHz
• Semi-angle of half power	~ 60º
• Transmit power	5 w
• DC bias	0.8 A
Camera	
• Frame rate f_c	50 fps
• f_s	200 Hz
• f_h	10 KHz
• Aperture	f/3.5
• Focal length	18-135 mm
• Shutter speed	1/4000 s
• Image sensor size	22.4×15 mm
ANN structure	
• Neuron number of input layer	2
• Hidden layer number and neuron number	1×15
• Neuron number of output layer	2
Room size	0.85×0.85×1.85 m

Table II. Comparison of the VLC based positioning systems

Works	Methods used	PE	Room size	Positioning type
Ref. [8]	TDOA	9.2 cm	1.2×1.2×2 m	2D
Ref. [9]	RSS/Carrier allocation	2.4 cm	0.6×0.6×0.6 m	2D
Ref. [15]	Image processing	6 cm	1×1×0.8 m	3D
Ref. [16]	Image processing	6 cm	0.5×0.5×1.2 m	2D
Proposed Scheme	Image processing	~1 cm	0.85×0.85×1.85 m	2D

Table III. Effect of tilted angle

Tilted angle (degree)	PE (cm)
0	0.8
5.7	16.9
15.5	38.8
-5.7	17.1
-15.5	36.4

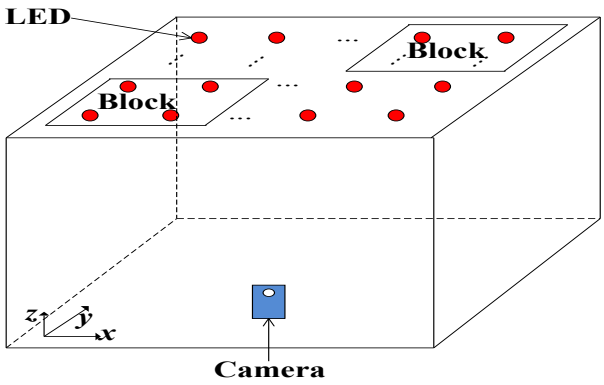

Fig. 1 System block diagram.

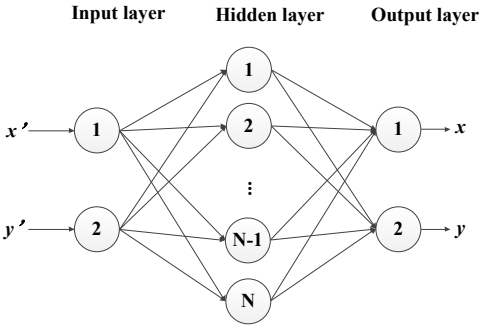

Fig. 2 Structure of an artificial neural network.

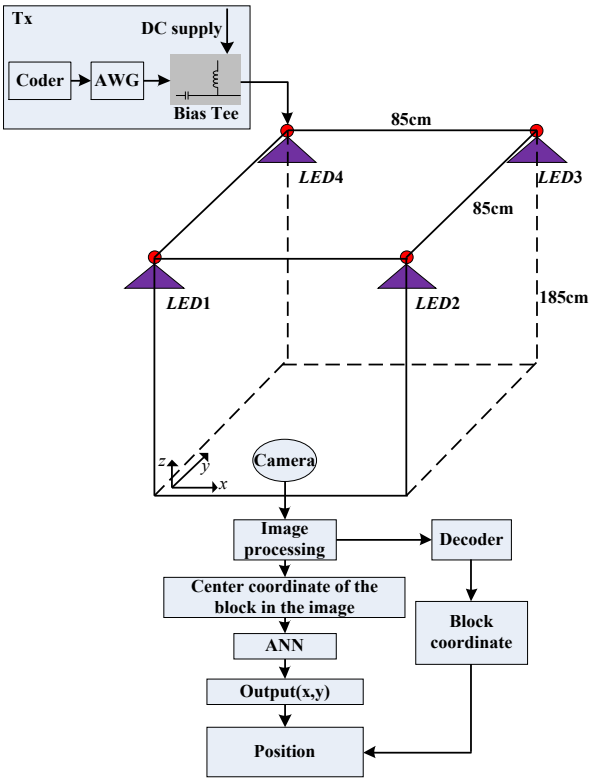

Fig. 3 Experiment setup for the proposed IPS based on OCC and ANN.

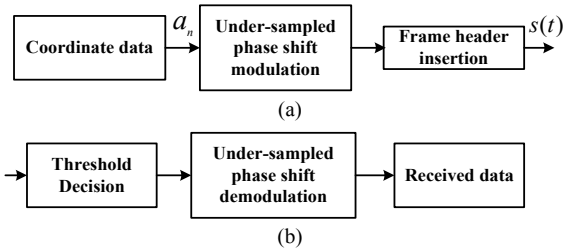

Fig. 4. Block diagram of: (a) coder, and (b) decoder.

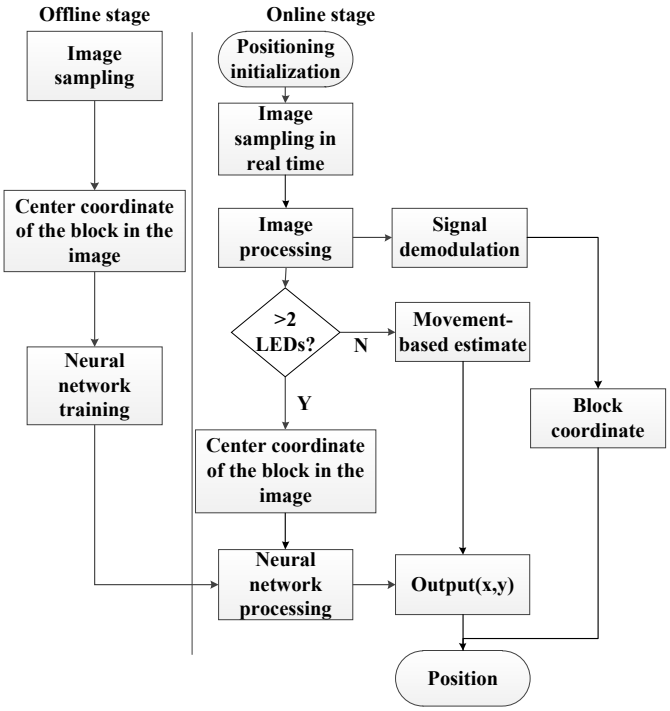

Fig. 5. The flow chart for determining the position in the proposed system.

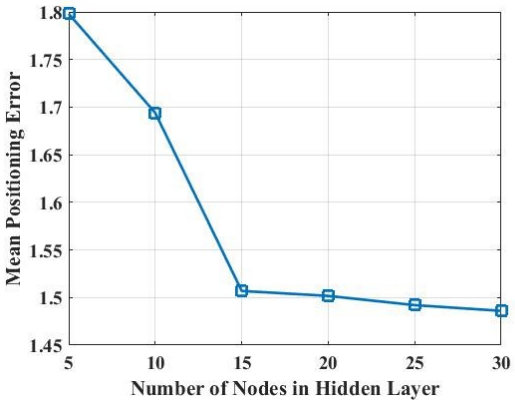

Fig. 6. The mean PE versus the number of nodes in the hidden layer.

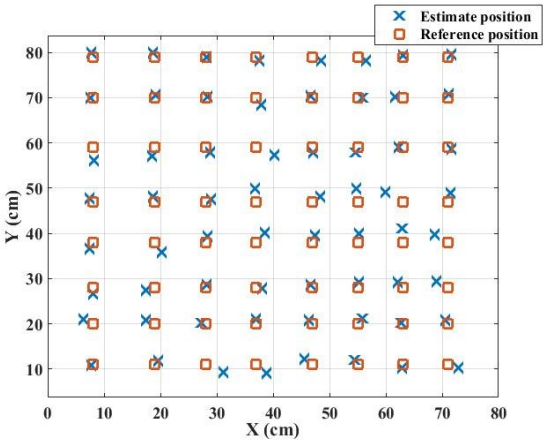

Fig. 7. The final estimated positions using our proposed scheme.